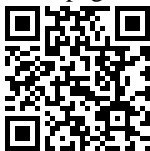


Scientific Inquiry and Review (SIR)

Volume 9 Issue 1, 2025


ISSN(P): 2521-2427, ISSN(E): 2521-2435

Homepage: <https://journals.umt.edu.pk/index.php/SIR>



Article QR



- Title:** Polymeric Rod-shaped Lanthanum Oxide Nanoparticles Generated from Polygonum Minus Leaf Extract: Synthesis, Characterization, and Antioxidant Activities
- Author (s):** Mariam Achakzai¹, Aziza Sarwar¹, Muhammad Nawaz¹, Karimah Kassim², Ehsanullah Kakar³, Muhammad Rasool¹, and Sajjad Bhangward⁴
- Affiliation (s):** ¹Balochistan University of Information Technology, Engineering and Management Sciences, Quetta, Pakistan
²Universiti Teknologi Mara, Selangor, Malaysia
³University of Loralai, Loralai, Pakistan.
⁴Quaid-e-Awam University of Engineering, Science and Technology, Nawabshah, Pakistan.
- DOI:** <https://doi.org/10.32350/sir.91.03>
- History:** Received: June 22, 2024, Revised: August 18, 2025, Accepted: September 10, 2025, Published: June 10, 2025
- Citation:** Achakzai M, Sarwar A, Nawaz M, et al. Polymeric Rod-shaped lanthanum oxide nanoparticles generated from Polygonum minus leaf extract: synthesis, characterization, and antioxidant activities. *Sci Inq Rev.* 2025;9(1):01–10. <https://doi.org/10.32350/sir.91.03>
- Copyright:** © The Authors
- Licensing:**  This article is open access and is distributed under the terms of [Creative Commons Attribution 4.0 International License](https://creativecommons.org/licenses/by/4.0/)
- Conflict of Interest:** Author(s) declared no conflict of interest



UMT

A publication of
The School of Science
University of Management and Technology, Lahore, Pakistan

Polymeric Rod-shaped Lanthanum Oxide Nanoparticles Generated from *Polygonum Minus* Leaf Extract: Synthesis, Characterization, and Antioxidant Activities

Abstract

The need to synthesise metal nanoparticles has emerged in recent years due to their wide range of applications in various biological activities. This study reports a facile and rapid synthesis of biogenic lanthanum nanoparticles using *Polygonum minus* leaf extract as reducing agent. The reduction of La^{+3} to elemental La rapidly occurred and was completed within 10 minutes at room temperature. Moreover, the size of nanoparticles is highly sensitive to leaf extract concentration and pH. The synthesized nanoparticles were characterized using Fourier transform infra-red (FT-IR), energy dispersive X-ray diffraction (EDX), field emission scanning electron microscopy (FE-SEM), powder X-ray diffraction (PXRD), and UV-Visible (Uv-Vis) spectroscopy. The FTIR analysis of the La_2O_3 NPs confirmed the presence of characteristic La-O band at 614 cm^{-1} . The band of La_2O_3 NPs was observed in the range of 300-400 nm in Uv-Vis spectrum, which further affirmed its successful synthesis. The EDAX analysis confirmed the presence of La in the produced nanoparticles. FESEM showed them as elongated rod-like structure with a uniform particle size of about 343 nm, determined by image J software and confirming their rod-like morphology. The virtual broad band in the XRD pattern revealed the lack of a periodic crystal structure, implying that the produced nanoparticles were entirely amorphous. The TG-DTA results showed their thermal stability. Further, the nanoparticles were subjected to antioxidant activity using DPPH assay. The results revealed that La_2O_3 NPs exhibited 28.3% inhibition. The synthesized nanoparticles open new frontiers for various other biological applications.

Keywords: antioxidant activity, biogenic, La_2O_3 NPs, polymeric, rod shaped

1. Introduction

In recent decades, green synthesis of metal oxide nanoparticles has been studied broadly due to their high surface to volume ratio. Among the other metal oxide nanoparticles, the oxides of rare-earth elements show various fascinating characteristics, including a high number of active sites, significant structural stability, as well as superior optical, magnetic, and chemical capabilities [1]. The lanthanoids-based nanoparticles garner a lot of attention due to their wide range of uses in biomedicine, chemical industry, and agriculture and material sciences [2]. In addition, lanthanoids

can also be applied in X-ray tomography imaging, near infrared (NIR) imaging, single-photon emission computed tomography (SPECT), biosensing, and antioxidant therapy [3].

Numerous methodologies and protocols are available for the synthesis of La_2O_3 NPs, including solvothermal, hydrothermal, chemical precipitation, and green synthesis. Among these, green synthesis provides environmentally friendly products by removing or reducing the harmful substances [4]. Green nanotechnology scholars have studied the synthesis of nanoparticles thoroughly using various microorganisms, such as algae, fungi, bacteria, and viruses [5]. Moreover, metal oxide nanoparticles produced using plant extracts have useful practical applications [6]. The several silver oxide NPs produced using *tridax procumbens* and *cluster bean* extracts are used as biosensors, revealing their high antimicrobial activity [7]. Furthermore, platinum oxide NPs obtained from the *holy basil* extract are used for catalytic activity [8]. Moreover, lanthanum nanoparticles produced using *multingia calabura* leaves extract are used for antibacterial activity against *Staphylococcus aureus* and *Escherichia coli*. These nanoparticles exhibit good anticoagulant, thrombolytic, and hemolytic activities with antioxidant inhibition of 70.06% [6]. In addition, lanthanum oxide nanoparticles (La_2O_3 NPs) produced by *Andrographis paniculata* leaf extract show promising antibacterial activity against *S. aureus* and *E. coli*, as well as anti-inflammatory and anticancerous properties [9]. La_2O_3 NPs produced using *Eucalyptus globulus* leaf extracts are very useful to control various inflammations and diabetic diseases [10]. Similarly, green synthesis of La_2O_3 NPs with the help of different plant extracts (*Physalis angulate*, *Datura metel*, *Muntingia calabura*, *Andrographis paniculate*, *Vigna radiata*, *Trigonella* and *foenum-graecum*) has remarkable applications in electronics, biomedicine, insulators, and biocatalysts [11].

Based on the aforementioned studies, plant-mediated synthesis of La_2O_3 NPs has received very little consideration by scientific community, although there is a broad scope for La_2O_3 NPs using various plant extracts. *Polygonum minus* extract has been used for the synthesis of noble metal nanoparticles (e.g., Au, Ag), although its application to rare-earth compounds, such as La_2O_3 NPs, remains novel. In this regard, the preparation of La_2O_3 NPs is a groundbreaking step toward making rare-earth nanoparticles in an environmentally friendly way. This method makes use of the extract's flavonoid, phenolic acid, and terpene content as dual-purpose agents [12], allowing for the near-complete reduction of La^{2+} ions in 10 minutes at room temperature. This improves the efficiency of the synthesis by removing the need for energy-intensive procedures, such as high

pressure or temperature. Additionally, by avoiding dangerous chemicals like NaBH_4 or organic solvents, reducing waste production, and producing biocompatible, low-cytotoxic NPs appropriate for biomedical applications—as demonstrated by smaller ecological footprints in similar green syntheses—it also supports environmental sustainability [13]. This approach not only lowers pollution and energy use but also conforms to eco-friendly nanotechnology principles, creating opportunities for the economical, scalable manufacture of rare-earth NPs with a negligible environmental impact. Hence, the current study focuses on the synthesis of La_2O_3 NPs using *P. minus* leaf extract. The synthesized nanoparticles are further investigated for their antioxidant activities.

2. Materials, Methods, and Instrumentation

2.1. Materials

All the chemicals employed in the research were of analytical grade and purchased through suppliers. Lanthanum (III) nitrate hexahydrate ($\text{La}(\text{NO}_3)_3 \cdot 6\text{H}_2\text{O}$) was obtained from Sigma-Aldrich. Whereas, fresh leaves of *P. minus* were purchased from a local market of Malaysia.

2.2. Instrumentation

The synthesized La_2O_3 NPs were characterized using various analytical techniques including UV-Vis spectroscopy, in the range of 400–800 nm, using Ultra-3000 series spectrophotometer. The amorphous structure of La_2O_3 NPs was determined by XRD (D2 Phaser from BRUKER Germany model A26-X1-A2B0B2A0). While, the FTIR analysis of La_2O_3 NPs was carried out via Perkin Elmer Spectrometer 1600, in the region of 400–4000 cm^{-1} , by using standard KBr pellet technique. The presence of elemental lanthanum, as well as its morphology, was determined by using EDX coupled with FESEM (Thermo Scientific model Apreo 2s). The average particle size was determined with the help of image j software. Thermal activity (TGA) was determined in a nitrogen atmosphere with a heating rate of 10°C/min using TA instruments Q50 TGA analyzer.

2.3. Preparation of Plant Extract Solution

A total of 1.0 g of *P. minus* leaf powder dried in an oven at 35°C was boiled in 50 ml of de-ionized water for 15 minutes before filtration. The filtered extract was refrigerated at 4°C. This extract was employed as a reducing and stabilizing agent in the preparation of nanoparticles.

2.4. Preparation of Lanthanum Salt Solution

Approximately 1mM solution of lanthanum (III) nitrate hexahydrate ($\text{La}(\text{NO}_3)_3 \cdot 6\text{H}_2\text{O}$) was prepared by adding 0.01 g of lanthanum salt in 30 ml of de-ionized water.

2.5. Synthesis of Lanthanum Oxide Nanoparticles

A total of 9 ml leaf extract solution was added dropwise into the salt solution (30 ml; 1 mM). The mixture was stirred for 20 mins. The resulting solution was centrifuged at 16000 rpm for another 20 mins. The resultant pellets were re-dispersed into de-ionized water and methanol after the supernatants were discarded. To get rid of any impurities adsorbed on the surface of La_2O_3 NPs, the centrifugation procedure was repeated two to three times and the powder was dried in a hot air oven at 45°C.

2.6. Antioxidant Activity

Antioxidants are chemicals, either natural or artificial, that stop or postpone cell damage brought on by oxidants. Any chemical that delays, stops, or eliminates oxidative damage in the target molecule is an antioxidant. The chemical must be active at low radical concentrations in order to be regarded as an antioxidant. Its amount must be sufficient to deactivate the target molecule. Further, it must react with oxygen or nitrogen free radicals and the final product of the reaction must be less toxic than the removed radical. Phenolic antioxidants frequently lose their activity at high concentrations and act as prooxidants. Various antioxidants interact with diverse reactive species in a variety of ways at different sites, while defending certain biological targets [13, 14].

2.6.1. Preparation of Samples for Antioxidant Activity

For antioxidant activity, three different types of stock solutions were prepared including La_2O_3 NPs and DPPH solutions, as well as ascorbic acid solution. The free radical scavenging activity of La_2O_3 NPs and conventional ascorbic acid was tested using the stable radical DPPH (0.004g/100ml methanol) solution. Approximately 5mg/ml of La_2O_3 NPs and a similar amount of ascorbic acid at various concentrations (10, 20, 30, 50, 100, and 200 mg/ml) were vortexed violently with 3 ml

freshly produced DPPH solution. The solution was then incubated at room temperature in the dark for 30 minutes. A Uv-Vis spectrophotometer at 517 nm was used to measure absorption. DPPH was used as control, while methanol was used as blank solution [14].

$$\text{Scavenging\%} = \frac{H_c - H_s}{H_c} \times 100$$

Here, H_c is the absorbance of control (DPPH) and H_s is the absorbance of La_2O_3 NPs / ascorbic acid.

3. Results and Discussion

3.1. Uv-Visible Analysis

The size, shape, and morphology of La_2O_3 NPs are greatly influenced by a number of factors, including pH, temperature, reaction time, and concentration. Their synthesis and stability between 200-800 nm were evaluated using a Shimadzu spectrophotometer [15].

3.1.1 Time Dependent Studies

Fig. 2 displays the absorption spectra of La_2O_3 NPs synthesized using 1 mm lanthanum salt solution and 9 ml *P. minus* leaf extract, measured at various time intervals. A stable absorption peak at 300-400 nm indicates successful NP synthesis, with no significant change in intensity over two weeks, confirming the long-term stability of the La_2O_3 NPs [16].

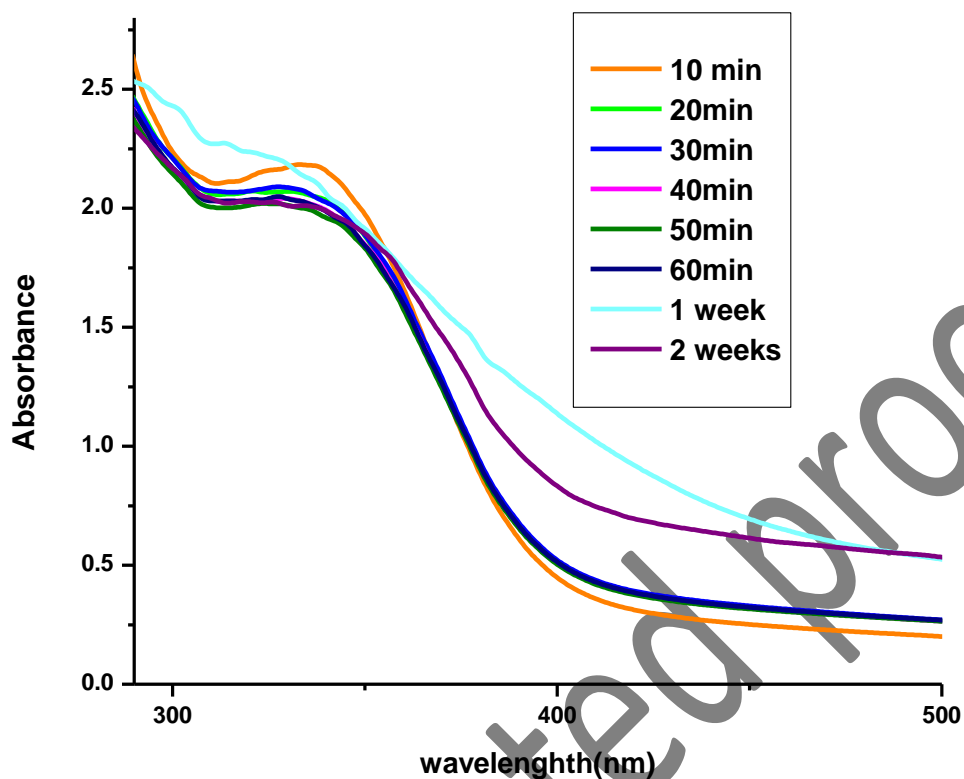


Figure 2. UV-Vis Absorption Spectra of La_2O_3 NPs Over Time

Concentration Dependent Studies

The effects of the concentrations of leaf extract and salt solution [17] are depicted in **Figs. 3a and 3b**, respectively. **Fig 3a** shows the effects of 9, 18, and 27 ml leaf extract concentrations on (1 mm) salt solution. As the amount of leaf extract increased, a gradual decrease was observed in the peak of La_2O_3 NPs, as evident by the Uv-Vis spectra of the resulting particles. It was found that adding 9 ml of leaf extract to the reaction mixture was successful in producing La_2O_3 NPs. Uv-Vis spectra showed that the sharpness of the absorption peak is dependent on the leaf extract concentration, thus the peak was sharper at 9 ml. However, with the increase in leaf extract red shift was recorded, indicating an increase in particle size [16].

Furthermore, **Fig 3b** shows the effects of 1, 2, and 3 mm salt solutions respectively on 9 ml of leaf extract in the synthesis of La_2O_3 NPs. It was noticed that all the selected concentrations were

effective in the synthesis of La_2O_3 NPs and a clear band was observed at 308 nm [17]. Hence, it was proved that the concentration of leaf extract can affect synthesis La_2O_3 NPs production, as compared to the concentration of salt solution.

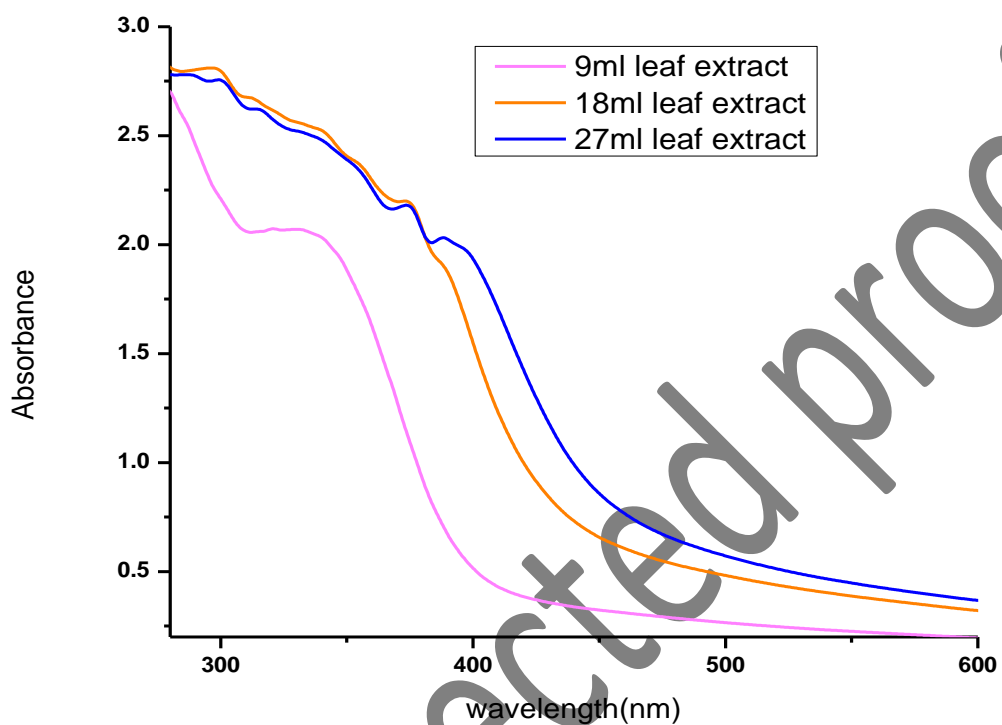


Figure 3a. UV-Vis Spectra Showing the Effects of Leaf Extract Concentration on La_2O_3 NP Synthesis

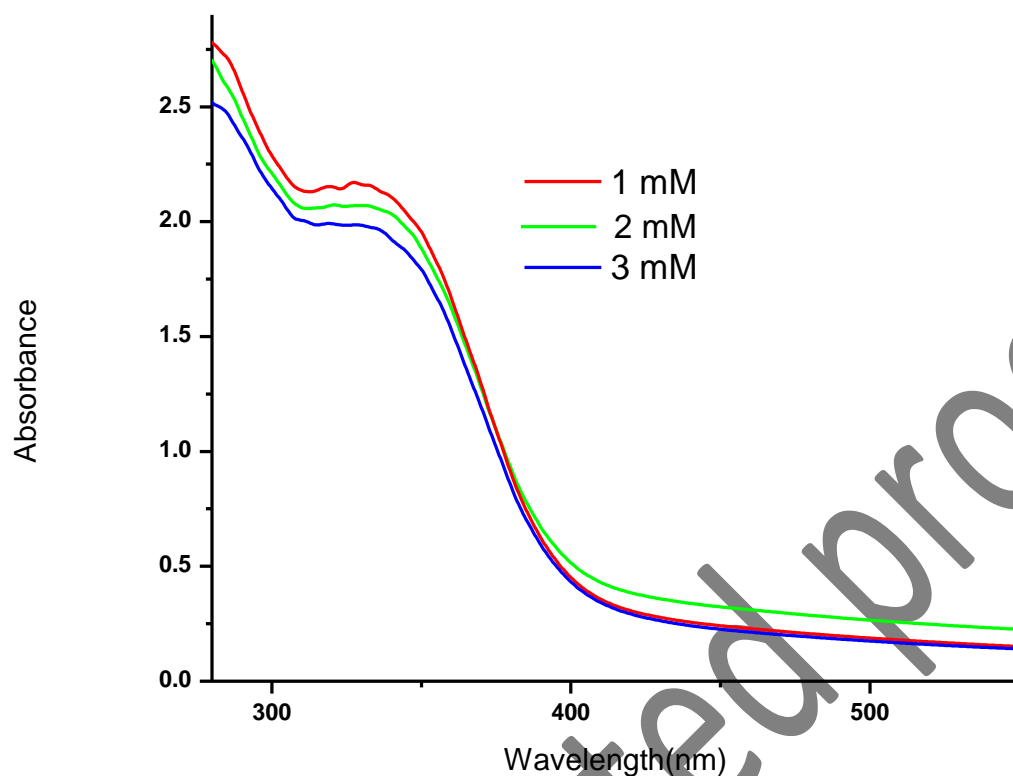


Figure 3b. UV-Vis Spectra Showing the Effects of Lanthanum Salt Concentration on La_2O_3 NP Synthesis

3.1.3. Temperature Dependent Studies

The size and morphology of La_2O_3 NPs were greatly affected by the reaction temperature. **Fig 4** depicts the absorption spectra of La_2O_3 NPs produced at varied temperatures, ranging from room temperature to 80°C . Notably, the absorption peak and wavelength did not change with an increase in temperature. It was fascinating to see that synthesized La_2O_3 NPs remained extremely stable, even at a high temperature [16].

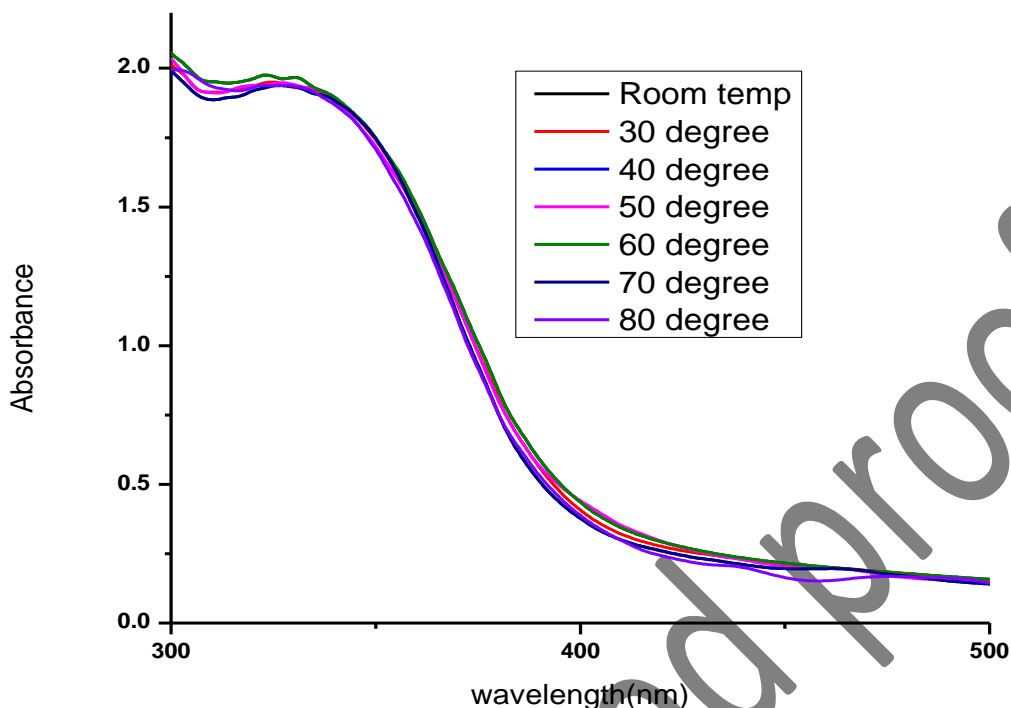


Figure 4. UV-Vis Spectra of La_2O_3 NPs at Different Temperatures (RT to 80°C)

3.1.4. pH Dependent Studies

The pH is another important factor which affects the size, shape, and morphology of the synthesized La_2O_3 NPs. The electrical charges of biomolecules can alter as pH changes, which may have an impact on their reducing ability, capping ability, and growth [18]. The impact of both acidic and basic pH on the absorption spectra of the synthesized La_2O_3 NPs is depicted in **Figs. 5a and 5b**. **Fig 5a** reveals that when the pH dropped, a clear band of nanoparticles was seen even at the lowest pH. Whereas, **Fig 5b** shows that a rise in pH caused the absorption peak to shift towards a longer wavelength (from 308 to 450 nm), indicating that the size of the La_2O_3 NPs produced increased while their production decreased, suggesting the existence of larger particles with a polydispersed distribution. This may partially be due to the reaction of sodium hydroxide and the impact of acidic phenolic groups on flavonoids in the extract. Such an increase in particle size, coupled with an increase in the pH value, has been reported previously [19-21]. Therefore, the production of La_2O_3 NPs is more favored by an acidic pH as compared to a basic pH.

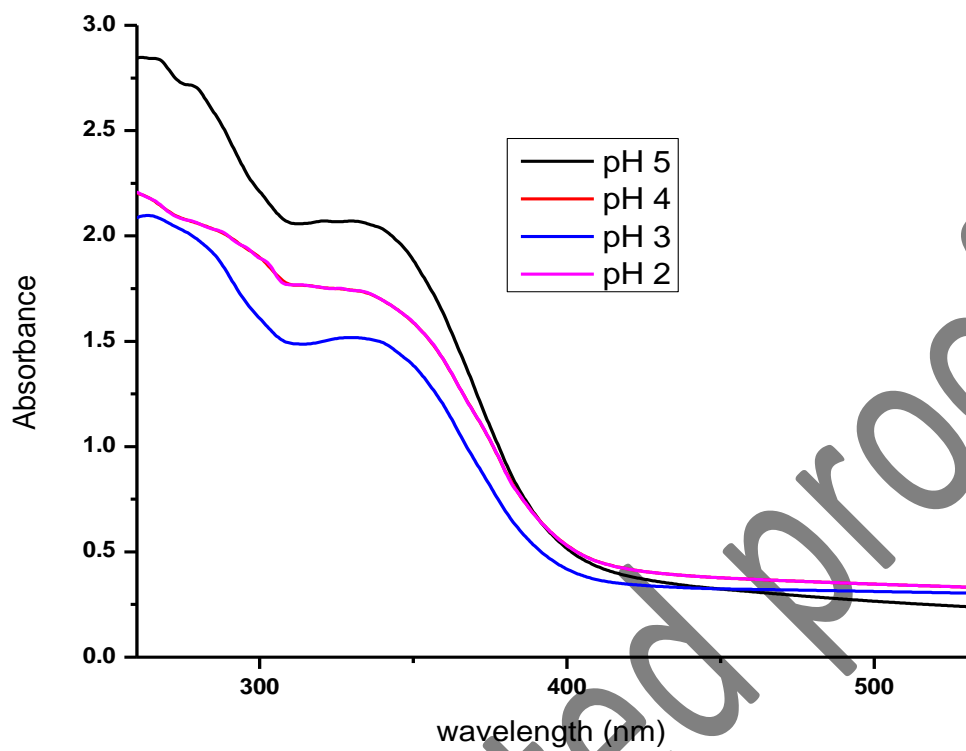


Figure 5a. UV-Vis Spectra of La_2O_3 NPs at Various Acidic pH Levels

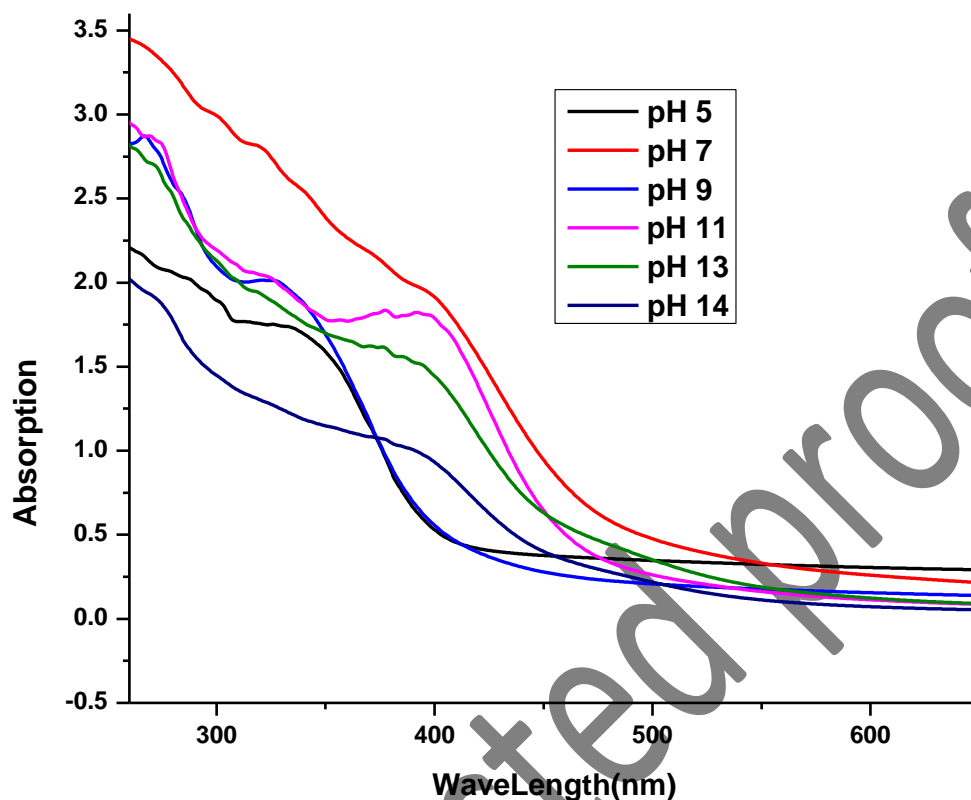


Figure 5b. UV-Vis Spectra of La₂O₃ NPs at Various Basic pH Levels

3.2. EDX Analysis

The purity and weight percentage of the produced nanoparticles was confirmed by using the energy dispersive X-ray spectrometer. **Fig 6** shows a representative EDX spectrum. Several peaks of La can be distinguished in addition to the signals for O and P. The observed O and La peaks are related to La₂O₃ NPs. The presence of P was extract-derived and no toxic elements were detected, as reported earlier [22, 23].

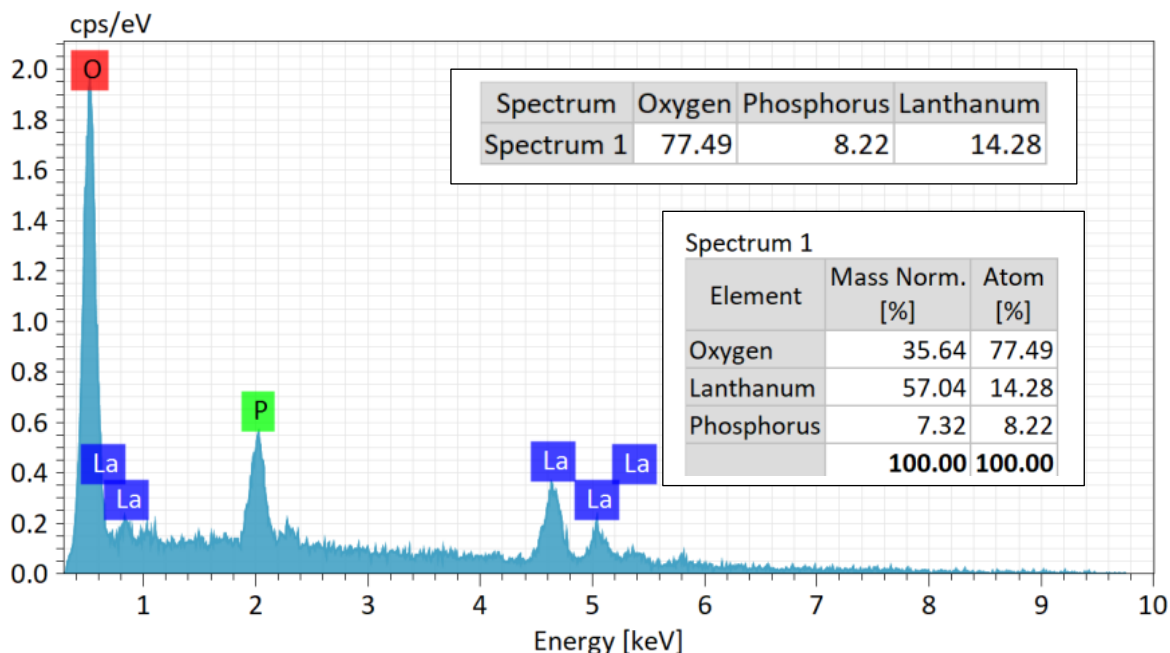


Figure 6. EDX Spectrum of La_2O_3 NPs

3.3. Powder X-ray Diffraction Analysis

P-XRD is used to determine amorphous nature and phase purity. The virtual broadband in the XRD pattern reveals the lack of periodic crystal structure in the amorphous sample, implying that the produced sample is entirely amorphous, as shown in **Fig 7**. It can be deduced that the synthesized La_2O_3 NPs exhibited a typical amorphous phase, as reported in the literature, while the crystallite size was not applicable for this study due to the lack of sharp crystalline peaks [24, 25]. This amorphous character, also observed in other biosynthesized metal oxide nanoparticles [25], may contribute to their enhanced surface reactivity. This is advantageous for antioxidant activity, as amorphous structures often provide more active sites for radical scavenging, as compared to their crystalline counterparts [6]. These results underscore the potential of *P. minus*-mediated La_2O_3 NPs for biomedical applications, particularly in antioxidant therapies.

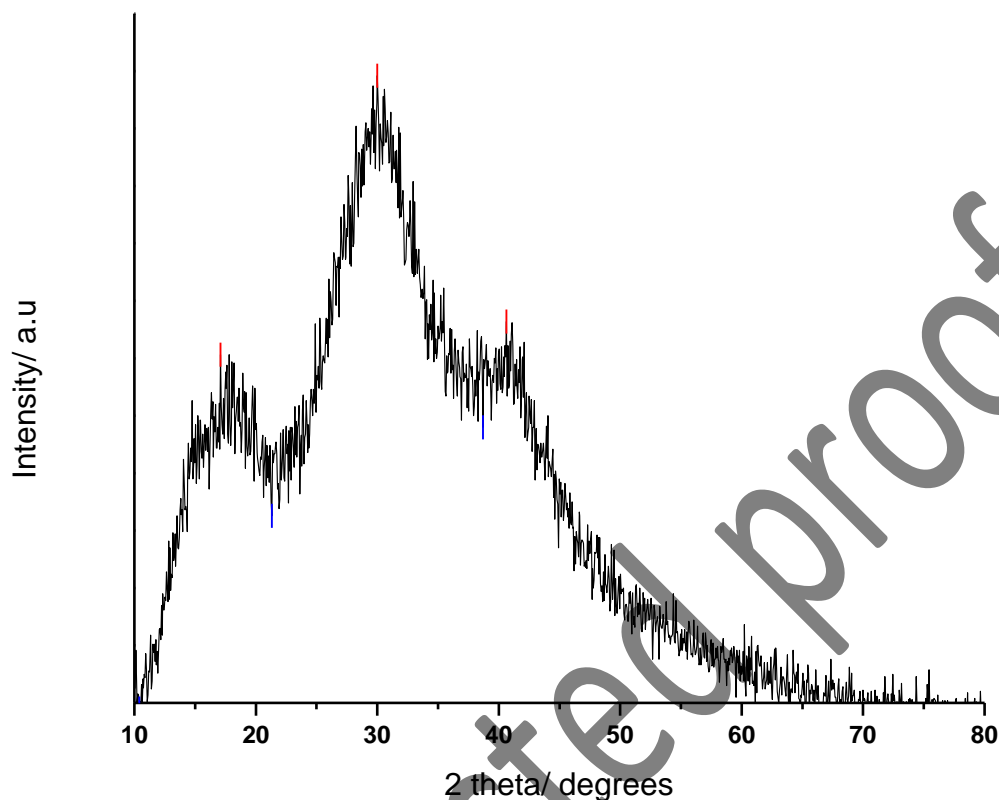


Figure 7. Powder XRD Pattern of La_2O_3 NPs

3.4. FE-SEM Studies

The size and surface morphology of La_2O_3 NPs were observed using FE-SEM. The images of La_2O_3 NPs are given in **Fig 8a**. It is clear that these nanoparticles are elongated and rod-like in their shape. They have a uniform particle size of about 343 nm, determined by image J software and shown in histogram (**Fig 8b**), confirming a rod-like morphology and polydispersity. Polymeric nanoparticles are particles measuring between 1-1000 nm in size. They showed a significant potential for targeted drug delivery during the treatment of various medical conditions. Moreover, they can also be used for a variety of antibacterial, antifungal, and cytotoxic purposes [26-29].

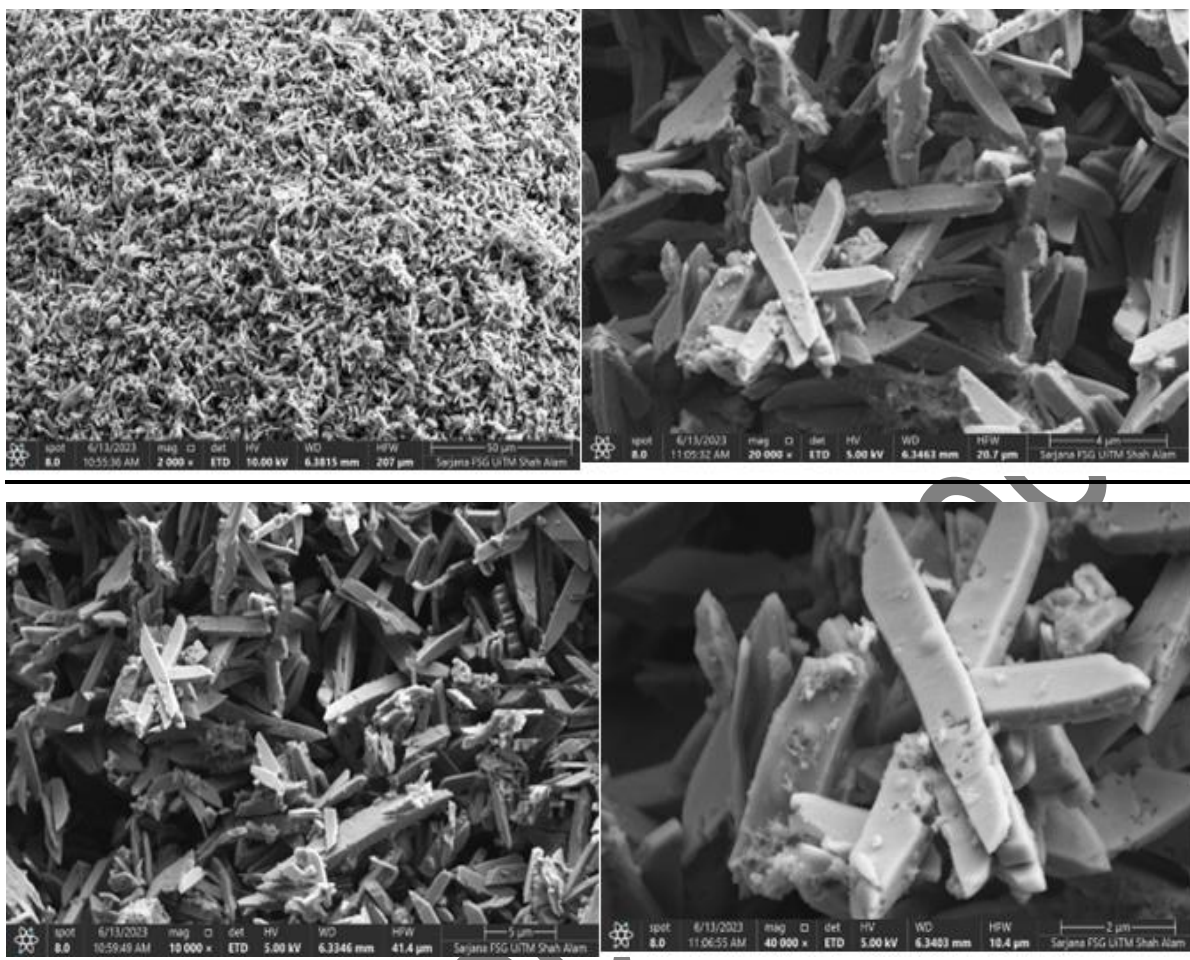


Figure 8a. FE-SEM Images of La_2O_3 NPs

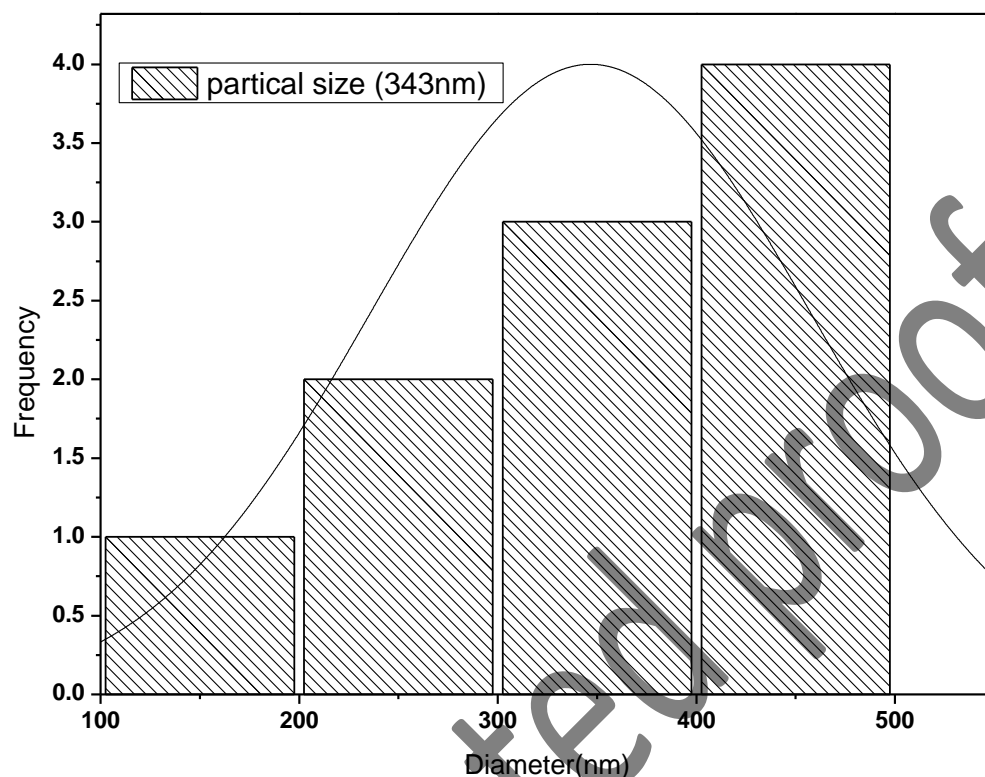


Figure 8b. Particle Size Distribution Histogram of La₂O₃ NPs

3.5. FTIR Analysis

The FTIR analysis was carried out to identify the possible functional groups of biomolecules present in the *P. minus* leaf. These biomolecules are responsible for the reduction of La (NO₃)₃·6H₂O to elemental lanthanum and stabilization of the formed La₂O₃ NPs. FTIR spectra of the *P. minus* leaf powder and the synthesized La₂O₃NPs, using 9 ml of *P. minus* extract at pH 5, is shown below in **Fig 9a**. The FTIR spectrum of leaf powder showed characteristic bands for O-H stretching vibrations at 3428 cm⁻¹ (polyols), stretching vibrations of C=O at 1638cm⁻¹ (unsaturated carbonyl group), and stretching vibrations of C-O at 1068 cm⁻¹ (polyols) [30,31]. The asymmetric stretching vibrations of C-H at 2924 cm⁻¹, as well as the stretching vibrations of CHO at 1625 cm⁻¹, confirmed the presence of phenolic compounds including flavonoids (quercetin and myricetin) in the *P. minus* leaf aqueous extract, as reported earlier [32].

Absorption sharp band clearly observed at 614 cm^{-1} is attributable to La-O stretching vibration, as depicted in **Fig 9b**, confirming the successful synthesis of La_2O_3 NPs [33, 34]. This observation suggests the likely involvement of the flavonoids of the *P. minus* leaf extract in the bio reduction process of La^{+3} to $\text{La} (0)$, stabilizing the La_2O_3 NPs [35]. The presence of these bioactive molecules on the surface of nanoparticles likely enhanced their biocompatibility and contributed to their moderate antioxidant activity (28% DPPH scavenging at $200\text{ }\mu\text{g/ml}$), since phenolic compounds are known to donate electrons to neutralize free radicals, a mechanism supported by research on plant-mediated nanoparticle synthesis [17].

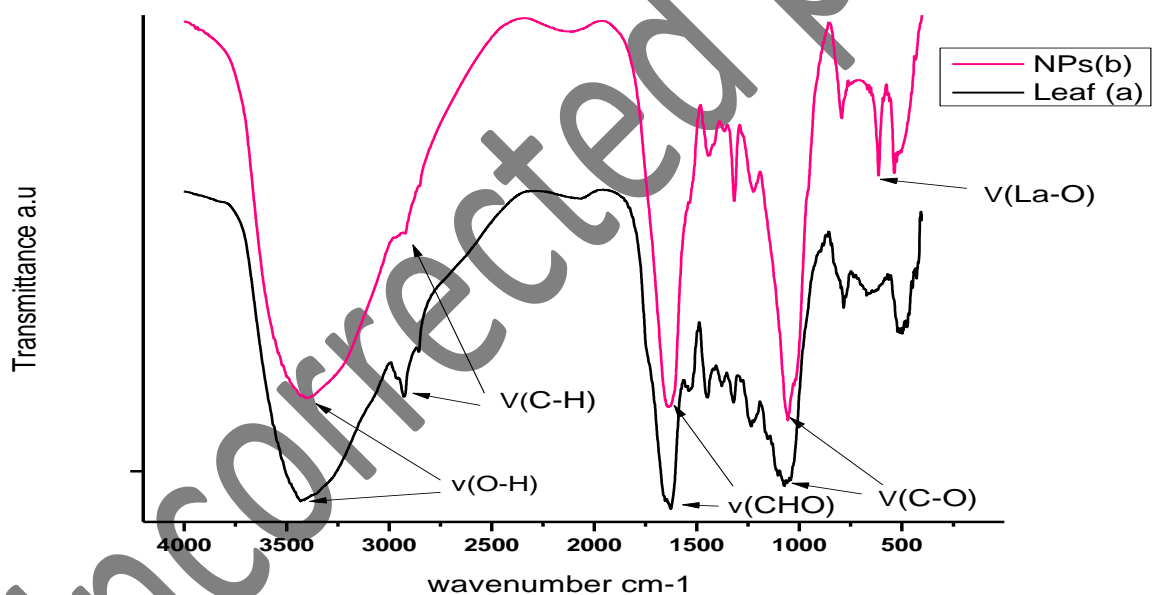


Figure 9a. FTIR Spectra of *P. minus* Leaf Powder and Synthesized La_2O_3 NPs

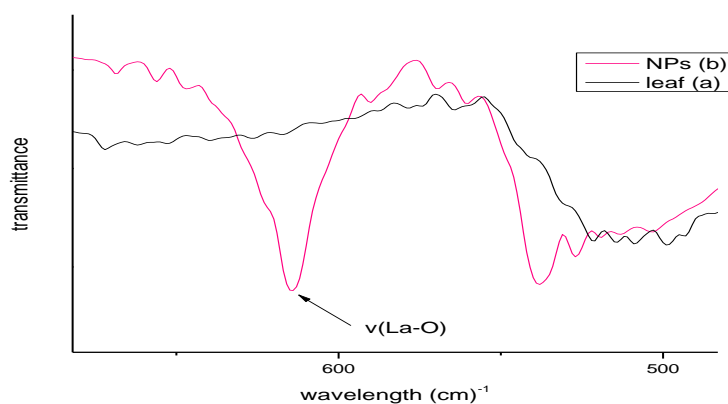


Figure 9b. FTIR Spectra Showing La-O Band in La_2O_3 NPs

3.6. Thermal Gravimetric Analysis

Thermal studies were performed to investigate lanthanum nanoparticles, where thermogravimetric analysis was executed within the temperature range of ambient to 900°C . Thermal stability is regarded as a remarkable property of La_2O_3 NPs. Thermal curves of the compounds are given below in **Fig 10**. La_2O_3 NPs decomposed thermally in 3 main steps. Firstly, the weight loss of 10% in the temperature range $70\text{--}191^\circ\text{C}$, with the DTA temperature of 75°C , is attributable to the loss of crystal water. Secondly, a further decay through the combustion of organic moieties with a weight loss of 53% was observed at the temperature range of $191\text{--}380^\circ\text{C}$, with the DTA temperature of 388°C . Finally, decomposition occurred with the residual mass of 46% at the DTA temperature of 815°C . This thermal stability, as reported in similar studies [33], indicates that the organic capping agents from *P. minus* enhance the nanoparticles' structural integrity, which is crucial for their application in biological environments where thermal and chemical stability are required.

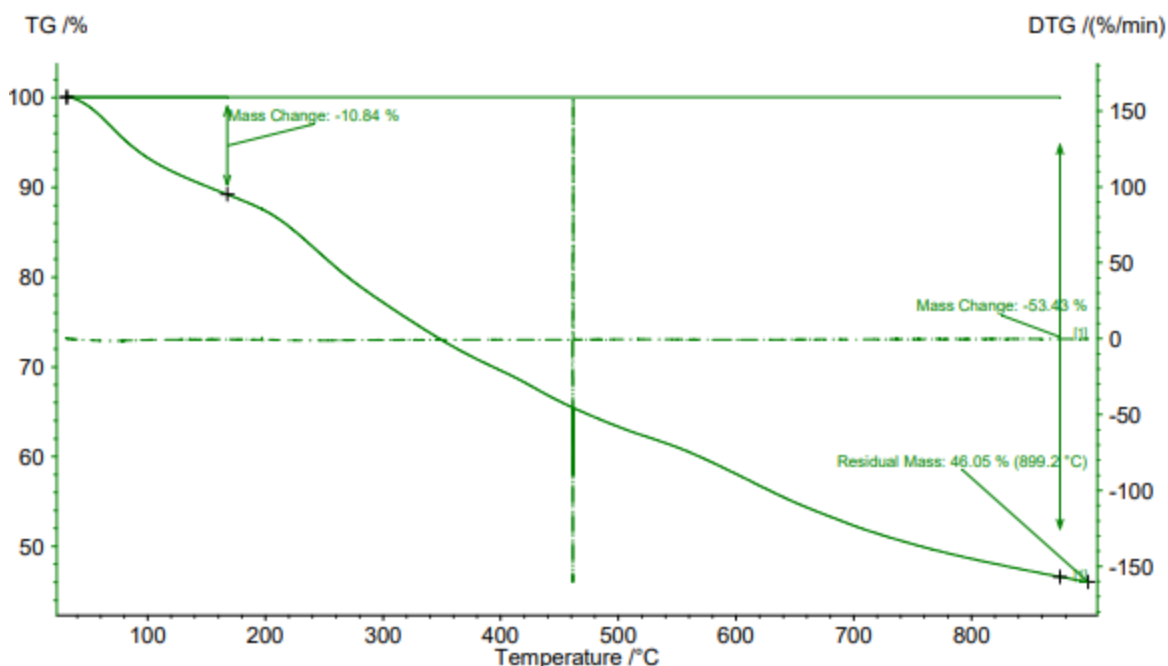


Figure 10. TGA/DTA Curves of La_2O_3 NPs

3.7. Antioxidant Activities

DPPH radical scavenging assay 2,2-diphenyl-1-picrylhydrazyl is a stable free synthetic radical at room temperature. Further, by accepting an electron or hydrogen radical, it becomes a stable molecule. In the DPPH assay, antioxidants reduced the DPPH radical to the non-radical form. Hence, absorption was reduced and the color of the DPPH solution changed from purple to yellow. This is known as scavenging and it can be done only by an antioxidant. In the current study, when the sample was subjected to DPPH, 28% of scavenging occurred. The DPPH scavenging of the La_2O_3 NPs confirmed its antioxidant nature. Lanthanum nanoparticles showed antioxidant activity but less than standard ascorbic acid, as observed in **Figs. 11a** and **b**.

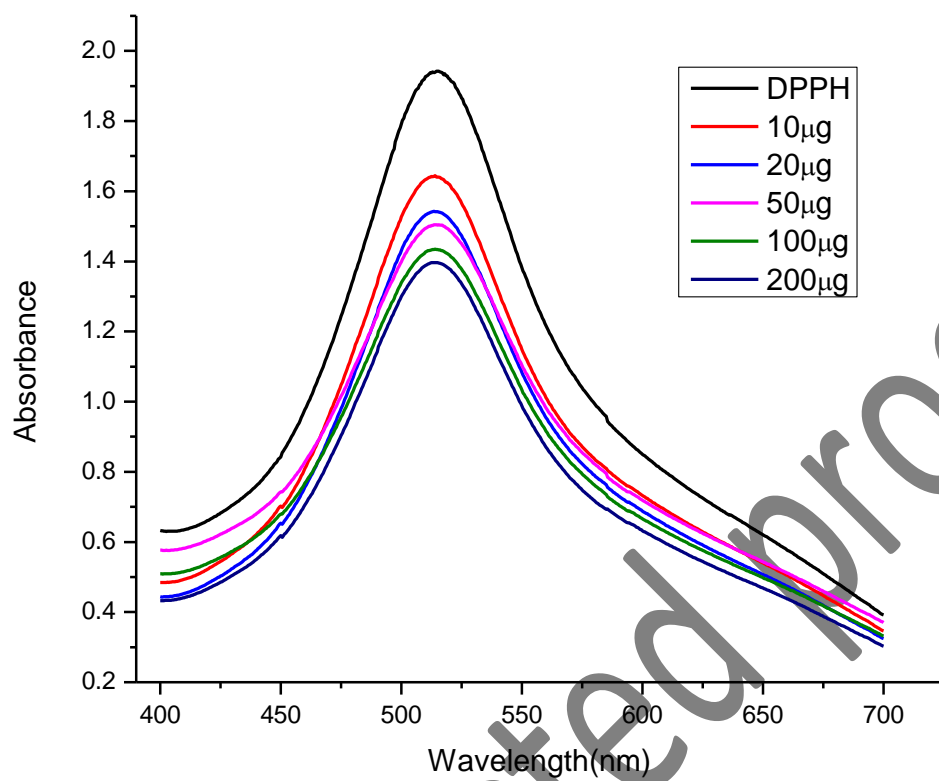


Figure 11a. DPPH Scavenging Activity of La_2O_3 NPs

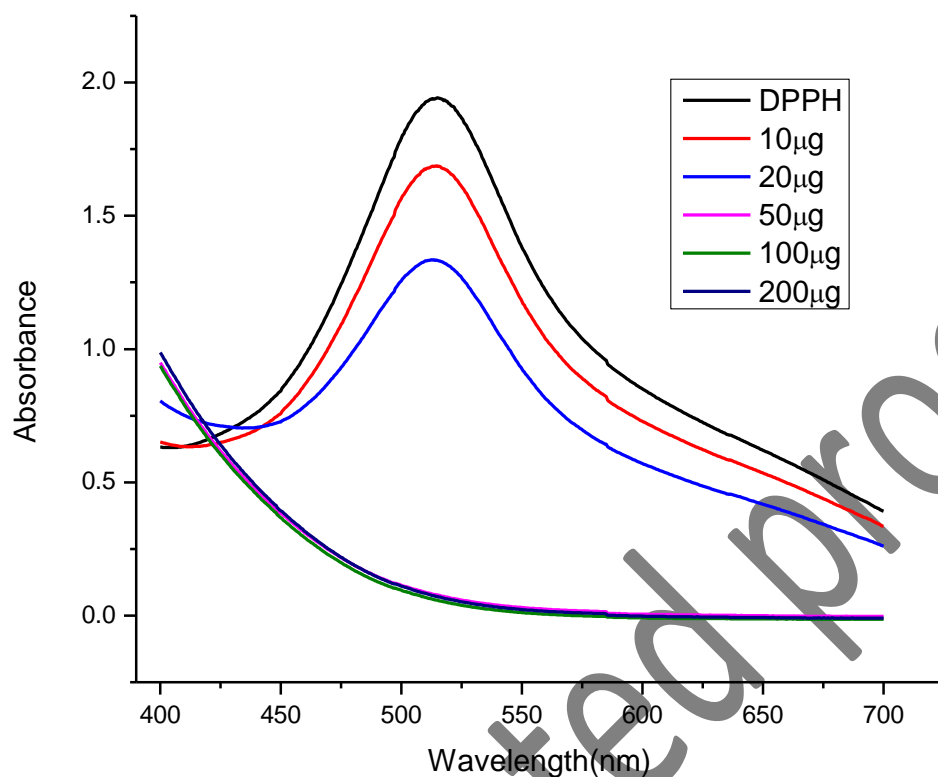


Figure 11b. DPPH Scavenging Activity of Ascorbic Acid

The percentage of free radical scavenging activity of various samples at different concentrations ranging from 10 to 200 µg/ml for standard ascorbic acid is shown below in **Fig 12** [36].

La_2O_3 NPs, synthesized by *P. minus*, exhibited a DPPH scavenging activity of 28% at 200 µg/ml, demonstrating moderate antioxidant potential. This performance is comparably moderate as compared to other nanoparticles synthesized by different plant extracts, as reported in the literature. For instance, among plant-mediated lanthanum NPs, those synthesized using *Muntingia calabura*-derived lanthanum NPs showed a scavenging activity of 70.06% at 5 mg/ml. Similarly, silver nanoparticles synthesized from *Petiveria alliacea L.* leaf extract displayed antioxidant activity ranging from 61.39% to 70.69% at 5 mg/ml [6].

Scavenging activity depends on the quality and quantity of the antioxidant (nanoparticles). As stated above, La_2O_3 NPs showed moderate quality as compared to other nanoparticles mentioned

above. The antioxidant activity of lanthanum nanoparticles may be attributed to bioactive chemicals, primarily polyphenols, that are coated on them. According to early reports, lanthanum nanoparticles made from plant extracts have antioxidant properties and their antioxidant nature grows as their concentration rises. Hence, if the concentration of La_2O_3 NPs increases, its antioxidant activity may gradually increase as well [6].

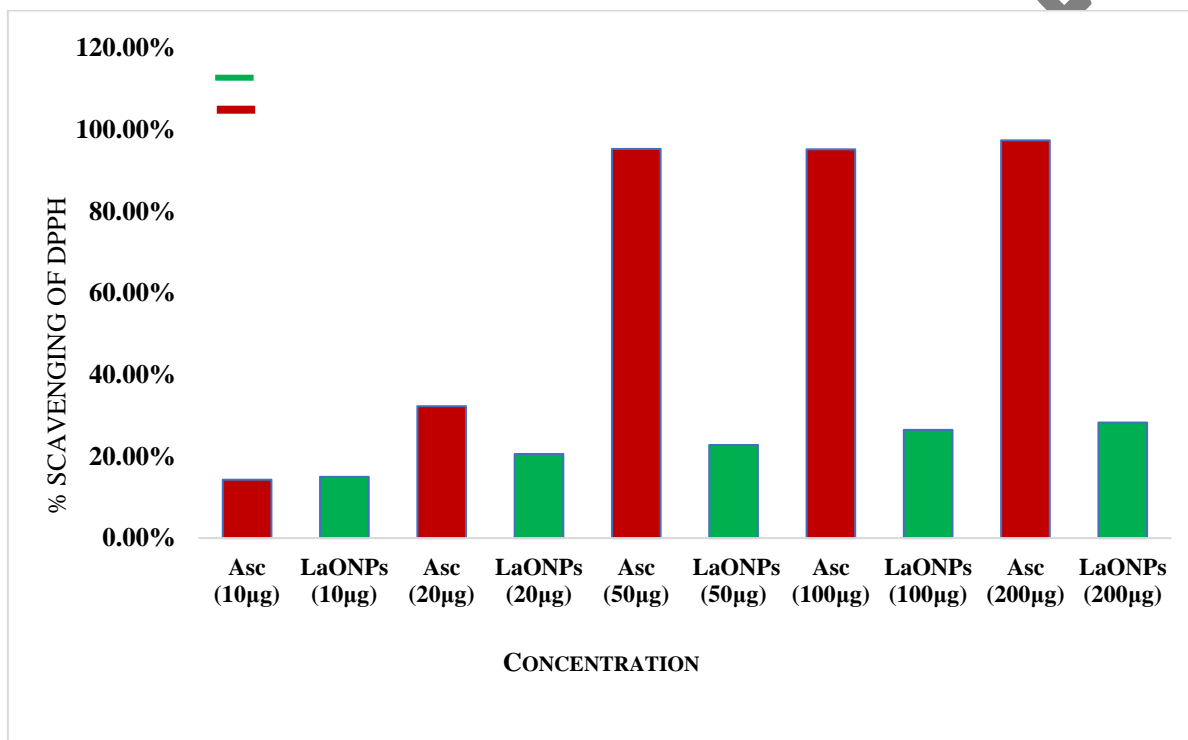


Figure 12. DPPH Scavenging Percentages for La_2O_3 NPs and Ascorbic Acid

The study revealed that at the concentration of $200\mu\text{g/ml}$, La_2O_3 NPs showed greater antioxidant activity by scavenging 28% DPPH but less than ascorbic acid, that is, 97%. Percentage scavenging of DPPH revealed the potency of the sample towards its antioxidant activity.

Table 1 shows the DPPH scavenging ability of lanthanum nanoparticles and ascorbic acid at varied concentrations.

Table 1. DPPH Scavenging Percentages at Various Concentrations

Samples	Methanol	DPPH	Absorbance	% Scavenging of DPPH
Ascorbic acid (10 µg/ml)	990 µl	3 ml	1.66	14.3%
Ascorbic acid (20 µg/ml)	980 µl	3 ml	1.31	32.3%
Ascorbic acid (50 µg/ml)	950 µl	3 ml	0.09	95.3%
Ascorbic acid (100 µg/ml)	900 µl	3 ml	0.06	95.2%
Ascorbic acid (200 µg/ml)	800 µl	3 ml	0.05	97.4%
NPs (10 µg/ml)	990 µl	3 ml	1.644	15%
NPs (20 µg/ml)	980 µl	3 ml	1.537	20.6%
NPs (50 µg/ml)	950 µl	3 ml	1.494	22.8%
NPs (100 µg/ml)	900 µl	3 ml	1.422	26.5%
NPs (200 µg/ml)	800 µl	3 ml	1.388	28.3%

Conclusion

This research established a simple and easy technique of synthesizing polymeric La₂O₃ NPs from the aqueous extract of *P. minus*. The effect of temperature, reaction time, concentration, and pH on La₂O₃ NPs were analyzed by Uv-Vis spectroscopy. A clear band of La-O nanoparticles at 308 nm was observed. The peaks in the FTIR spectra indicated the potential role of different functional groups of plant metabolites as capping and stabilizing agents, while nanoparticles showed the characteristic band of La-O at 614 cm⁻¹. The size of the synthesized nanoparticles was 343 nm, as determined by image J software. EDAX analysis confirmed the presence of lanthanum along with oxides and phosphorus. While, XRD pattern confirmed the amorphous nature of lanthanum nanoparticles. Further, TG-DTA analysis was performed to investigate the thermal properties of La₂O₃ NPs. The synthesized La₂O₃ NPs were found to exhibit moderate antioxidant activity. It can be concluded that further *in vitro* and *in vivo* explorations can fully assess the biomedical applicability of these synthesized polymeric nanoparticles, particularly in areas such as imaging, sensing, therapy, and antimicrobial activities, as demonstrated in biocompatibility assessments and potential applications of lanthanide nanomaterials.

Future Direction

Future research should concentrate on thorough *in vitro* studies to assess the biocompatibility, cytotoxicity, and potential biomedical applications of polymeric lanthanum oxide nanoparticles (La₂O₃ NPs) synthesized using *P. minus* leaf extract, including targeted drug delivery and antimicrobial activity. Investigating different plant extracts with rich phytochemical profiles, such as *Ocimum sanctum* or *Azadirachta indica*, may improve the manufacturing process, as well as the stability and bioactivity of nanoparticles.

Data Availability

All data generated and analyzed during this study are included in this article.

Conflict of Interest

The authors declare that they have no known competing financial interests or personal relationships that could have appeared to influence the work reported in this paper.

Compliance with Ethical Standards

Funding

Not Applicable

References

1. Sulaiman N, Yulizar Y, Apriandanu DOB. Eco-friendly method for synthesis of La₂O₃ nanoparticles using *Physalis angulata* leaf extract. AIP Conf Proc. 2018;(October 2018):1–6. <https://doi.org/10.1063/1.5064102>
2. Hollande E, Lebugle A. Europium-doped bioapatite: a new photostable biological probe, internalizable by human cells. Biomater. 2003;24:3365–3371. [https://doi.org/10.1016/S0142-9612\(03\)00169-8](https://doi.org/10.1016/S0142-9612(03)00169-8)
3. Balusamy B, et al. Characterization and bacterial toxicity of lanthanum oxide bulk and nanoparticles. J Rare Earths. 2012;30(12):1298–1302. [https://doi.org/10.1016/S1002-0721\(12\)602245](https://doi.org/10.1016/S1002-0721(12)602245)
4. Moothedan M, Sherly KB. Synthesis, characterization and sorption studies of nano lanthanum oxide. J Water Process Eng. 2016;9:29–37. <https://doi.org/10.1016/j.jwpe.2015.11.002>
5. Akhtar MS, Panwar J, Yun YS. Biogenic synthesis of metallic nanoparticles by plant extracts. ACS Sustain Chem Eng. 2013;1(6):591–602. <https://doi.org/10.1021/sc300118u>
6. Manoj KA, et al. Biogenic synthesis, characterization and biological activity of lanthanum nanoparticles. Mater Today Proc. 2020;21:887–895. <https://doi.org/10.1016/j.matpr.2019.07.727>
7. Narayanan KB, Sakthivel N. Green synthesis of biogenic metal nanoparticles by terrestrial and aquatic phototrophic and heterotrophic eukaryotes and biocompatible agents. Adv Colloid Interface Sci. 2011;169(2):59–79. <https://doi.org/10.1016/j.cis.2011.08.004>
8. Zheng H, et al. Hydrothermal synthesis of various shape-controlled europium hydroxides. Nanomater. 2021;11(2):1–10. <https://doi.org/10.3390/nano11020529>
9. Veerasingam M, Murugesan B, Mahalingam S. Ionic liquid mediated morphologically improved lanthanum oxide nanoparticles by *Andrographis paniculata* leaves extract and its biomedical applications. J Rare Earths. 2020;38(3):281–291. <https://doi.org/10.1016/j.jre.2019.06.006>
10. Maheshwaran G, et al. Eco-friendly synthesis of lanthanum oxide nanoparticles by *Eucalyptus globulus* leaf extracts for effective biomedical applications. Mater Lett. 2021;283(1):128799. <https://doi.org/10.1016/j.matlet.2020.128799>

11. Dabhane H, et al. Plant mediated green synthesis of lanthanum oxide (La₂O₃) nanoparticles: a review. Asian J Nanosci Mater. 2020;3(November):291–299. <https://doi.org/10.26655/AJNANOMAT.2020.4.3>
12. Mian KH, Mohamed S. Flavonoid (myricetin, quercetin, kaempferol, luteolin, and apigenin) content of edible tropical plants. J Agric Food Chem. 2001;49(6):3106–3112. <https://doi.org/10.1021/jf000892m>
13. Ingale AG, Chaudhari AN. Biogenic synthesis of nanoparticles and potential applications: an ecofriendly approach. J Nanomed Nanotechnol. 2013;4(2):1–7. <https://doi.org/10.4172/2157-7439.1000165>
14. Shameli K, et al. Green biosynthesis of silver nanoparticles using Callicarpa maingayi stem bark extraction. Molecules. 2012;17(7):8506–8517. <https://doi.org/10.3390/molecules17078506>
15. Bhakya S, et al. Biogenic synthesis of silver nanoparticles and their antioxidant and antibacterial activity. Appl Nanosci. 2016;6(5):755–766. <https://doi.org/10.1007/s13204-015-0473-z>
16. Saware K, Venkataraman A. Biosynthesis and characterization of stable silver nanoparticles using Ficus religiosa leaf extract: a mechanism perspective. J Clust Sci. 2014;25(4):1157–1171. <https://doi.org/10.1007/s10876-014-0697-1>
17. Jain S, Mehata MS. Medicinal plant leaf extract and pure flavonoid mediated green synthesis of silver nanoparticles and their enhanced antibacterial property. Sci Rep. 2017;7(1):1–13. <https://doi.org/10.1038/s41598-017-15724-8>
18. Dwivedi AD, Gopal K. Biosynthesis of silver and gold nanoparticles using Chenopodium album leaf extract. Colloids Surf A Physicochem Eng Asp. 2010;369(1–3):27–33. <https://doi.org/10.1016/j.colsurfa.2010.07.020>
19. Liu B, et al. Optimization of high-yield biological synthesis of single-crystalline gold nanoplates. J Phys Chem B. 2005;109(32):15256–15263. <https://doi.org/10.1021/jp051449n>
20. Panáček A, et al. Silver colloid nanoparticles: synthesis, characterization, and their antibacterial activity. J Phys Chem B. 2006;110(33):16248–16253. <https://doi.org/10.1021/jp063826h>

21. Noruzi M, Zare D, Davoodi D. A rapid biosynthesis route for the preparation of gold nanoparticles by aqueous extract of cypress leaves at room temperature. *Spectrochim Acta A Mol Biomol Spectrosc.* 2012;84–88. <https://doi.org/10.1016/j.saa.2012.03.041>
22. Diallo A, et al. Green synthesis of CO₃O₄ nanoparticles via *Aspalathus linearis*: physical properties. *Green Chem Lett Rev.* 2015;8(3–4):30–36. <https://doi.org/10.1080/17518253.2015.1082646>
23. Thema FT, et al. Green synthesis of ZnO nanoparticles via *Agathosma betulina* natural extract. *Mater Lett.* 2015;161:124–127. <https://doi.org/10.1016/j.matlet.2015.08.052>
24. Xing J, et al. High-efficiency light-emitting diodes of organometal halide perovskite amorphous nanoparticles. *ACS Nano.* 2016;10(7):6623–6630. <https://doi.org/10.1021/acsnano.6b01540>
25. Hoang V, Ganguli D. Amorphous nanoparticles - experiments and computer simulations. *Phys Rep.* 2012;518(3):81–140. <https://doi.org/10.1016/j.physrep.2012.07.004>
26. Khan I, Saeed K, Khan I. Nanoparticles: properties, applications and toxicities. *Arab J Chem.* 2019;12(7):908–931. <https://doi.org/10.1016/j.arabjc.2017.05.011>
27. Lee H, et al. Molecularly self-assembled nucleic acid nanoparticles for targeted in vivo siRNA delivery. *Nat Nanotechnol.* 2012;7(6):389–393. <https://doi.org/10.1038/nnano.2012.73>
28. Zielinska A, et al. Polymeric nanoparticles: production, characterization, toxicology and ecotoxicology. *Molecules.* 2020;25(16). <https://doi.org/10.3390/molecules25163731>
29. Medina C, et al. Nanoparticles: pharmacological and toxicological significance. *Br J Pharmacol.* 2007;150(5):552–558. <https://doi.org/10.1038/sj.bjp.0707130>
30. Pocurull E, Marcé RM, Borrull F. Determination of phenolic compounds in natural waters by liquid chromatography with ultraviolet and electrochemical detection after on-line trace enrichment. *J Chromatogr A.* 1996;738(1):1–9. [https://doi.org/10.1016/0021-9673\(96\)00070-2](https://doi.org/10.1016/0021-9673(96)00070-2)
31. Dauthal P, Mukhopadhyay M. *Prunus domestica* fruit extract-mediated synthesis of gold nanoparticles and its catalytic activity for 4-nitrophenol reduction. *Ind Eng Chem Res.* 2012;51(40):13014–13020. <https://doi.org/10.1021/ie300369g>
32. Miean KH, Mohamed S. Flavonoid (myricetin, quercetin, kaempferol, luteolin, and apigenin) content of edible tropical plants. *J Agric Food Chem.* 2001;49:3106–3112.

33. Imanaka N, Masui T, Kato Y. Preparation of the cubic-type La_2O_3 phase by thermal decomposition of LaI_3 . *J Solid State Chem.* 2005;178(1):395–398. <https://doi.org/10.1016/j.jssc.2004.11.006>
34. Chakraborty P, Dam D, Abraham J. Bioactivity of lanthanum nanoparticle synthesized using *Trigonella foenum-graecum* seed extract. *J Pharm Sci Res.* 2016;8(11):1253–1257.
35. Borhamdin S, Shamsuddin M, Alizadeh A. Biostabilised icosahedral gold nanoparticles: synthesis, cyclic voltammetric studies and catalytic activity towards 4-nitrophenol reduction. *J Exp Nanosci.* 2016;11(7):518–530. <https://doi.org/10.1080/17458080.2015.1090021>
36. Singh J, Dhaliwal AS. Novel green synthesis and characterization of the antioxidant activity of silver nanoparticles prepared from *Nepeta leucophylla* root extract. *Anal Lett.* 2018;0(0):1–18. <https://doi.org/10.1080/00032719.2018.1454936>